J. Fluid Mech. (1973), *vol.* 57, *part* 3, *pp.* 417–431
Printed in Great Britain

A family of steady vortex rings

By J. NORBURY
Department of Mathematics, University College London

(Received 18 May 1972 and in revised form 23 October 1972)

Axisymmetric vortex rings which propagate steadily through an unbounded ideal fluid at rest at infinity are considered. The vorticity in the ring is proportional to the distance from the axis of symmetry. Recent theoretical work suggests the existence of a one-parameter family, $\sqrt{2} \geqslant \alpha > 0$ (the parameter α is taken as the non-dimensional mean core radius), of these vortex rings extending from Hill's spherical vortex, which has the parameter value $\alpha = \sqrt{2}$, to vortex rings of small cross-section, where $\alpha \rightarrow 0$. This paper gives a numerical description of vortex rings in this family. As well as the core boundary, propagation velocity and flux, various other properties of the vortex ring are given, including the circulation, fluid impulse and kinetic energy. This numerical description is then compared with asymptotic descriptions which can be found near both ends of the family, that is, when $\alpha \rightarrow \sqrt{2}$ and $\alpha \rightarrow 0$.

1. Introduction

The recent theoretical work of Fraenkel (1970) and Norbury (1972) renders the existence of a (conjectured) one-parameter family of steady vortex rings highly plausible. These vortex rings are axisymmetric and move without change of shape through an unbounded inviscid fluid of uniform density at rest at infinity. The vorticity in each ring is proportional to the distance from the axis of symmetry. The following sections give a numerical description of typical vortex rings in this family, which is characterized by the parameter α with $\sqrt{2} \geqslant \alpha > 0$. Here α is defined as the non-dimensional mean core radius. The family ranges from Hill's spherical vortex, which has the parameter value $\alpha = \sqrt{2}$, to vortex rings of small cross-section, where the parameter $\alpha \rightarrow 0$. This explicit numerical description will complement any non-constructive, global existence work for the family of vortex rings.

The constructive existence theories of Norbury (1972) and Fraenkel (1970) lead to approximate descriptions of those vortex rings for which $\alpha \rightarrow \sqrt{2}$ and $\alpha \rightarrow 0$. Asymptotic results for a vortex ring close to Hill's vortex are established in Norbury (1973), while the corresponding results for a vortex ring with small cross-section are given in Fraenkel (1972). The good agreement of the numerical and asymptotic results at appropriate values of α suggests (a) that the asymptotic results for $\alpha \rightarrow \sqrt{2}$ and $\alpha \rightarrow 0$ are useful approximations over large intervals $\sqrt{2} > \alpha \geqslant \alpha_1$ and $\alpha_2 \geqslant \alpha > 0$ respectively, and (b) that the numerical scheme does lead to correct approximations of the actual curves.

The essentials of the numerical scheme are as follows. The problem is first

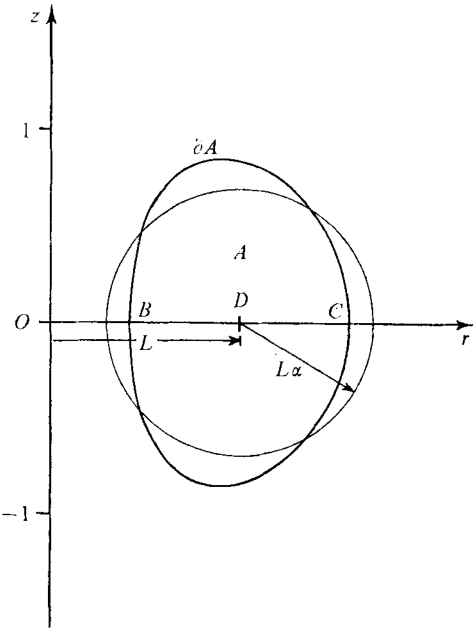

FIGURE 1. The meridional cross-section A of the vortex ring, specified by the parameter α ($= 0\cdot7$), with the ring radius $L = \frac{1}{2}(OB+OC)$. The core A, with boundary ∂A, has area $\pi L^2\alpha^2$. For this normalization the vorticity constant is $\Omega = U/L^2\alpha^2$, where U is a suitable reference velocity.

cast as a nonlinear integral equation for the boundary of the vortex ring. The boundary is represented by an appropriate Fourier series whose coefficients are found by an iterative process based on linearization of the integral equation about an initial guess.

This scheme also finds the propagation velocity and flux of the vortex ring. Then the fluid impulse, kinetic energy, circulation, volume of entrained fluid, etc., are found, and these results are given in § 3, where they are compared with the corresponding asymptotic results.

2. Formulation of the problem

2.1. *The integral equation for the core boundary*

As in Fraenkel (1970) and Norbury (1972) we start from the equations of continuity and vorticity for the steady axisymmetric flow, with no swirl, of an inviscid fluid of uniform density throughout space. The continuity equation, $\operatorname{div}\mathbf{v} = 0$, implies the existence of a vector potential $(0, \psi/r, 0)$ such that

$$\mathbf{v} = \operatorname{curl}(0, \psi/r, 0) = \left(-\frac{1}{r}\frac{\partial\psi}{\partial z}, 0, \frac{1}{r}\frac{\partial\psi}{\partial r}\right), \tag{2.1}$$

where $\psi(r,z)$ is the Stokes stream function, $\mathbf{v}$ the fluid velocity, and all components are with respect to cylindrical co-ordinates (r, λ, z). The vorticity equation,

$$\mathbf{v}.\operatorname{grad}(\omega/r) = 0, \tag{2.2}$$

is satisfied trivially by the particular distribution $\omega = \Omega r$, $\Omega =$ constant, of vorticity that we take in the core of each vortex ring in the family. We denote the meridional cross-section of the core by A (figure 1) and take axes fixed in the ring.

Then the problem can be stated: given the free-stream velocity W, the vorticity constant Ω, and a positive constant k, find the stream function ψ and the boundary ∂A of the core cross-section A such that

$$\left\{\frac{\partial^2}{\partial r^2} - \frac{1}{r}\frac{\partial}{\partial r} + \frac{\partial^2}{\partial z^2}\right\}\psi(r,z) = \begin{cases} -\Omega r^2 & \text{inside } \partial A, \\ 0 & \text{outside } \partial A \end{cases} \quad (2.3a)$$

(where we have taken the curl of (2.1)) and such that

$$\psi \text{ and grad } \psi \text{ are continuous across } \partial A, \quad (2.3b)$$

$$\psi = k \quad \text{on} \quad \partial A, \quad (2.3c)$$

$$\psi + \tfrac{1}{2}Wr^2 \to 0 \quad \text{as} \quad r^2 + z^2 \to \infty. \quad (2.3d)$$

Equations (2.3*b*, *c*) correspond to no flow of fluid through the boundary ∂A and to the continuity of tangential velocity across ∂A.

We observe that, if ∂A is assumed known, then ψ is given by

$$\psi(r,z) = -\tfrac{1}{2}Wr^2 + \frac{\Omega}{2\pi}\iint_A G(r,\hat{r},z-\hat{z})\,d\hat{r}\,d\hat{z}, \quad (2.4)$$

where
$$G(r,\hat{r},z-\hat{z}) = \tfrac{1}{2}r\hat{r}^2\int_{-\pi}^{\pi}\frac{\cos\hat{\lambda}\,d\hat{\lambda}}{\{r^2+\hat{r}^2-2r\hat{r}\cos\hat{\lambda}+(z-\hat{z})^2\}^{\frac{1}{2}}}. \quad (2.5)$$

Here (2.4) is based upon the fundamental solution $|\mathbf{x}-\hat{\mathbf{x}}|^{-1}$ of the Poisson equation satisfied by the vector potential. The kernel G is the stream function at $\mathbf{x} = (r,z)$ of a singular vortex circle at $\hat{\mathbf{x}} = (\hat{r},\hat{z})$ having vorticity of delta-function type with circulation $2\pi\hat{r}$.

Once ∂A is known, (2.4) represents the solution of the problem (2.3). So we combine (2.3*c*) and (2.4) to obtain the following nonlinear integral equation for the core boundary ∂A:

$$k = -\tfrac{1}{2}Wr^2 + \frac{\Omega}{2\pi}\iint_A G(r,\hat{r},z-\hat{z})\,d\hat{r}\,d\hat{z} \quad \text{for} \quad (r,z)\in\partial A. \quad (2.6)$$

The problem is thus reduced to finding curves ∂A that satisfy (2.6) for different W, Ω and k.

2.2. *An appropriate normalization of the integral equation*

First we seek a convenient representation for the curve ∂A. Thus we introduce the following non-dimensionalization. We refer all lengths to the ring radius L, defined as the distance from the axis $r = 0$ to the midpoint D of BC, the chord $z = 0$ of A (figure 1). The positive parameter α is introduced by

$$\text{area of } A = \pi L^2\alpha^2, \quad (2.7)$$

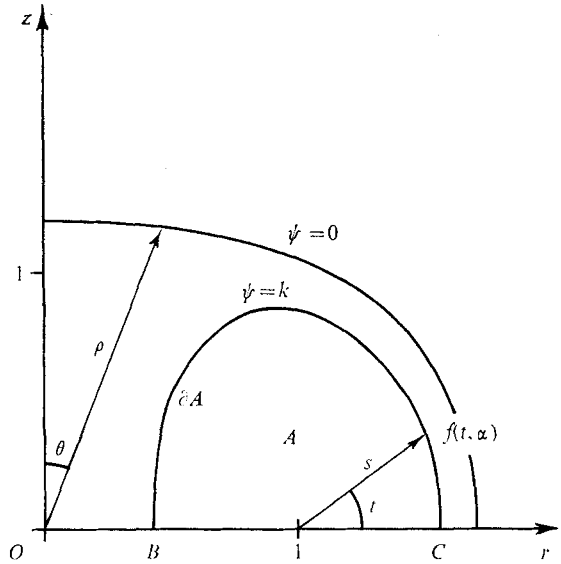

FIGURE 2. The core cross-section A with the boundary ∂A defined by $s = f(t, \alpha)$ in the (s, t) co-ordinates. The dividing streamline $\psi = 0$ is more appropriately defined in the usual (ρ, θ) spherical polar co-ordinates.

and is called the mean core radius. We choose a reference velocity U such that

$$\Omega = U/L^2\alpha^2 \tag{2.8}$$

is satisfied, and introduce non-dimensional variables $\bar{r}$, $\bar{z}$, $\overline{W}$, $\bar{k}$, etc., by

$$r = L\bar{r}, \quad z = L\bar{z}, \quad W = U\overline{W}, \quad k = UL^2\bar{k}, \quad \text{etc.} \tag{2.9}$$

We now consider Ω, L and α as given, rather than Ω, W and k, and thus solve (2.6) for k, W and ∂A. We do this to simplify the numerical and graphical work. Thus we consider the following form of (2.6), on dropping the bars after introducing the above non-dimensionalization:

$$k(\alpha) = -\tfrac{1}{2}W(\alpha)\,r^2 + \frac{1}{2\pi\alpha^2}\iint_{A(\alpha)} G(r, \hat{r}, z-\hat{z})\,d\hat{r}\,d\hat{z} \quad \text{for} \quad (r,z)\in\partial A(\alpha). \tag{2.10}$$

The area of A is $\pi\alpha^2$ and the midpoint of the chord $z = 0$ of A is $(1, 0)$. We find, for each $\alpha \in (0, \sqrt{2}]$ with this formulation of the problem, only one solution set $\{k, W, \partial A\}$ of (2.10).

We know a particularly simple solution of (2.10) for the parameter value $\alpha = \sqrt{2}$, that is, Hill's spherical vortex, when the constants have the values

$$k(\sqrt{2}) = 0, \quad W(\sqrt{2}) = \tfrac{4}{15}, \quad \partial A(\sqrt{2}) = \{(r,z)\,|\,r^2+z^2 = 4 \quad \text{or} \quad r = 0,\ |z| \leqslant 2\}. \tag{2.11}$$

Solutions of (2.10) have been found (Norbury 1972) for $\sqrt{2} \geqslant \alpha \geqslant \alpha_1$ (where α_1 is close to $\sqrt{2}$), with a different scaling. Solutions of (2.10) have also been found (Fraenkel 1970) for $\alpha_2 \geqslant \alpha > 0$ (where α_2 is small). Here we look for numerical solutions over the whole range $\sqrt{2} \geqslant \alpha > 0$. We introduce a new independent variable t so as to obtain a representation of the curves ∂A which is uniform over the whole range of α. Thus (s, t) co-ordinates are defined by (figure 2)

$$r = 1 + s\cos t \quad \text{and} \quad z = s\sin t,$$

and we look for symmetric curves $\partial A(\alpha)$ of the form

$$s = f(t, \alpha) = \sum_{n=0}^{\infty} a_n(\alpha)\cos nt. \tag{2.12}$$

(We note that G is a function of r, $\hat{r}$ and $|z - \hat{z}|$, so that ∂A will be symmetric.) In these co-ordinates (2.10) becomes, with $f \equiv f(t, \alpha)$ and $\hat{f} \equiv f(\hat{t}, \alpha)$.

$$k(\alpha) = -\tfrac{1}{2}W(\alpha)\{1 + f\cos t\}^2 + \frac{1}{2\pi\alpha^2}\int_0^{2\pi} d\hat{t} \times \int_0^{\hat{f}} G(1 + f\cos t, 1 + \hat{s}\cos\hat{t}, f\sin t - \hat{s}\sin\hat{t})\,\hat{s}\,d\hat{s} \quad (0 \leqslant t \leqslant \pi), \tag{2.13}$$

which we solve for k, W, a_2, a_3, ... for different $\alpha \in (0, \sqrt{2})$. We note that a_0 and a_1 are determined by the normalization. The condition that D is the midpoint of the chord BC implies that $s(0, \alpha) = s(\pi, \alpha)$; that is,

$$a_1 + a_3 + a_5 + \ldots = 0. \tag{2.14}$$

Hence a_1 is determined by the a_n, $n \geqslant 3$. The condition that the area of A is $\pi\alpha^2$ implies that

$$\begin{aligned}\pi\alpha^2 &= \int_0^{2\pi} d\hat{t}\int_0^{\hat{f}} \hat{s}\,d\hat{s},\\ &= \int_0^{2\pi} \tfrac{1}{2}\{a_0 + a_1\cos\hat{t} + a_2\cos 2\hat{t} + \ldots\}^2\,d\hat{t},\\ &= \pi\{a_0^2 + \tfrac{1}{2}(a_1^2 + a_2^2 + a_3^2 + \ldots)\}.\end{aligned} \tag{2.15}$$

Hence a_0 is determined from the a_n, $n \geqslant 1$.

2.3. *The numerical scheme*

For $\alpha \in (0, \sqrt{2}]$ we use the notation

$$P_\alpha(k, W, a_2, a_3, \ldots)(t) \equiv P_\alpha(\mathbf{X})(t) = 0 \quad (0 \leqslant t \leqslant \pi), \tag{2.16}$$

where $\mathbf{X} \equiv (X_1, X_2, X_3, X_4, \ldots) \equiv (k, W, a_2, a_3, \ldots)$ for the problem posed by equations (2.13)–(2.15). That is, given a suitable $\mathbf{X}$ and an $\alpha \in (0, \sqrt{2}]$, we first calculate $a_1(\mathbf{X})$ and $a_0(\mathbf{X}, \alpha)$ using (2.14) and (2.15), we then calculate $f(t, \alpha)$ using (2.12), and we finally define, using (2.13),

$$P_\alpha(\mathbf{X})(t) \equiv -X_1 - \tfrac{1}{2}X_2(1 + f\cos t)^2 + \frac{1}{2\pi\alpha^2}\int_0^{2\pi} d\hat{t} \times \int_0^{\hat{f}} G(1 + f\cos t, 1 + \hat{s}\cos\hat{t}, f\sin t - \hat{s}\sin\hat{t})\,\hat{s}\,d\hat{s} \quad (0 \leqslant t \leqslant \pi).$$

We note that X_1, $X_2 \geqslant 0$, and that our choice of X_3, X_4, ... is restricted by our desire to avoid the complications of having the curve $s = f(t, \alpha)$ intersect the axis $r = 0$. We bound X_3, X_4, ... by the corresponding Fourier coefficients of

Hill's spherical vortex (the first 40 are given in table 1 below). Our aim in the following is merely to render plausible the actual finite-dimensional approximation (2.19*) that we use to obtain numerical solutions to (2.13)–(2.15).

For a given $\alpha \in (0, \sqrt{2})$ let $\mathbf{X}^1$ be an initial approximation to the root of (2.16), and let $\boldsymbol{\delta}^*$ be the small difference $\mathbf{X} - \mathbf{X}^1$. Then, if P_α is differentiable with respect to $\mathbf{X}$ at $\mathbf{X}^1$, we can write

$$P_\alpha(\mathbf{X}) = P_\alpha(\mathbf{X}^1) + \sum_{j=1}^{\infty} \frac{\partial P_\alpha}{\partial X_j}(\mathbf{X}^1)\,\delta_j^* + R \quad (0 \leqslant t \leqslant \pi), \tag{2.17}$$

where the remainder R satisfies $|R|/|\boldsymbol{\delta}^*| \to 0$ as $|\boldsymbol{\delta}^*| \to 0$. Here $|\boldsymbol{\delta}^*|$ denotes the magnitude $\{\delta_1^{*2} + \delta_2^{*2} + \ldots\}^{\frac{1}{2}}$ of the vector $\boldsymbol{\delta}^*$. We solve the linear equation that follows from combining (2.16) and (2.17), and neglecting R; that is,

$$\sum_{j=1}^{\infty} \frac{\partial P_\alpha}{\partial X_j}(\mathbf{X}^1)\,\delta_j = -P_\alpha(\mathbf{X}^1) \quad (0 \leqslant t \leqslant \pi), \tag{2.18}$$

for $\boldsymbol{\delta}$. We observe that, if this linear equation has a unique solution $\boldsymbol{\delta}$, if the second derivatives $\partial P_\alpha/\partial X_i\,\partial X_j$ are bounded, and if the δ_i are sufficiently small, then $\mathbf{X}^2 = \mathbf{X}^1 + \boldsymbol{\delta}$ will be a better approximation to the solution of (2.16). In fact, under these conditions we know that $\mathbf{X}^n$ converges to the root of (2.16) as $n \to \infty$, where the successive approximations $\mathbf{X}^n$ $(n \geqslant 2)$ are calculated from the equations

$$\sum_{j=1}^{\infty} \frac{\partial P_\alpha}{\partial X_j}(\mathbf{X}^{n-1})\,\delta_j = -P_\alpha(\mathbf{X}^{n-1}) \quad (0 \leqslant t \leqslant \pi), \tag{2.19a}$$

$$\mathbf{X}^n = \mathbf{X}^{n-1} + \boldsymbol{\delta}. \tag{2.19b}$$

When P_α is differentiable this iterative scheme is just Newton's method applied to (2.16). We are unable to prove that this scheme converges, but have verified the convergence conditions numerically. In fact, we use the continuity of $\partial P_\alpha/\partial X_j$ in $\mathbf{X}$ to replace (2.19*a*) by

$$\sum_{j=1}^{\infty} \frac{\partial P_\alpha}{\partial X_j}(\mathbf{X}^1)\,\delta_j = -P_\alpha(\mathbf{X}^{n-1}) \quad (0 \leqslant t \leqslant \pi). \tag{2.19c}$$

We now replace (2.19*c*, *b*) by a finite-dimensional approximation. We use the notation $\bar{\mathbf{X}} = (X_1, \ldots, X_N)$. Then we consider

$$\left.\begin{aligned} \sum_{j=1}^{N} \frac{\partial P_\alpha}{\partial X_j}(\mathbf{X}^1)\,\delta_j &= -P_\alpha(\bar{\mathbf{X}}^{n-1}) \quad \text{for} \quad t = t_i \in [0, \pi] \quad (i = 1, \ldots, N), \\ \bar{\mathbf{X}}^n &= \bar{\mathbf{X}}^{n-1} + \bar{\boldsymbol{\delta}} \quad (n \geqslant 2). \end{aligned}\right\} \tag{2.19*}$$

Here we have forced the functional relation (2.19*c*) to hold only for N different points $t_i \in [0, \pi]$, so that we obtain a (hopefully well-posed) set of N simultaneous linear equations for the N unknowns $\delta_1, \ldots, \delta_N$. The success of this finite-dimensional approximation depends upon the appropriateness of the expansion (2.12) for the problem. We choose N so that the error in taking $a_n = 0$, $n \geqslant N$, is as small as the computational errors which occur in evaluating P_α, $\partial P_\alpha/\partial X_j$, etc.

Finally we need to approximate numerically the scheme (2.19*) to sufficient accuracy to ensure numerical convergence. Some of the computational details are given in the next section.

α ...	0·1	0·2	0·3	0·4	0·5	0·6	0·7	0·8
k	0·6804	0·4324	0·2967	0·2085	0·1469	0·1026	0·0704	0·0470
W	1·0195	0·8488	0·7402	0·6586	0·5922	0·5357	0·4863	0·4428
a_0	0·1000	0·1999	0·2997	0·3991	0·4978	0·5958	0·6928	0·7888
a_1	−0·0000	−0·0005	−0·0020	−0·0050	−0·0099	−0·0167	−0·0254	−0·0354
a_2	−0·0010	−0·0067	−0·0188	−0·0379	−0·0639	−0·0963	−0·1341	−0·1761
a_3	0·0000	0·0005	0·0022	0·0059	0·0122	0·0217	0·0344	0·0504
a_4	0·0000	0·0001	0·0007	0·0018	0·0040	0·0074	0·0120	0·0178
a_5	0·0000	−0·0000	−0·0002	−0·0009	−0·0026	−0·0057	−0·0109	−0·0184
a_6	—	—	0·0000	0·0001	0·0003	0·0008	0·0018	0·0035
a_7	—	—	0·0000	0·0001	0·0003	0·0008	0·0018	0·0035
a_8	—	—	—	−0·0000	−0·0001	−0·0005	−0·0012	−0·0027
a_9	—	—	—	0·0000	0·0000	0·0000	0·0001	0·0003
a_{10}	—	—	—	0·0000	0·0000	0·0001	0·0003	0·0008
a_{11}	—	—	—	0·0000	−0·0000	−0·0000	−0·0002	−0·0005
a_{12}	—	—	—	0·0000	—	—	0·0000	0·0000
a_{13}	—	—	—	−0·0000	—	—	0·0001	0·0002
a_{14}	—	—	—	—	—	—	—	−0·0001
a_{15}	—	—	—	—	—	—	—	0·0000
a_{16}	—	—	—	—	—	—	—	0·0000
a_{17}	—	—	—	—	—	—	—	0·0000

α ...	0·9	1·0	1·1	1·2	1·3	1·35	$\surd 2$	$\surd 2$ (a_{18}–a_{39})
k	0·0302	0·0182	0·0099	0·0044	0·0013	0·0004	0·0000	0·0085
W	0·4043	0·3703	0·3402	0·3136	0·2901	0·2793	0·2667	0·0060
a_0	0·8840	0·9783	1·0722	1·1659	1·2596	1·3066	1·3700	−0·0127
a_1	−0·0468	−0·0591	−0·0724	−0·0871	−0·1036	−0·1129	−0·1283	0·0063
a_2	−0·2208	−0·2665	−0·3116	−0·3542	−0·3921	−0·4083	−0·4276	0·0054
a_3	0·0692	0·0907	0·1145	0·1409	0·1702	0·1865	0·2129	−0·0105
a_4	0·0246	0·0318	0·0384	0·0429	0·0425	0·0391	0·0285	0·0048
a_5	−0·0284	−0·0410	−0·0558	−0·0723	−0·0895	−0·0981	−0·1099	0·0049
a_6	0·0061	0·0099	0·0154	0·0236	0·0361	0·0454	0·0643	−0·0089
a_7	0·0061	0·0091	0·0140	0·0184	0·0208	0·0200	0·0140	0·0038
a_8	−0·0053	−0·0092	−0·0149	−0·0228	−0·0332	−0·0399	−0·0508	0·0045
a_9	0·0006	0·0013	0·0025	0·0051	0·0112	0·0172	0·0313	−0·0077
a_{10}	0·0016	0·0032	0·0056	0·0087	0·0116	0·0123	0·0098	0·0031
a_{11}	−0·0011	−0·0024	−0·0047	−0·0086	−0·0154	−0·0209	−0·0307	0·0042
a_{12}	0·0000	0·0000	0·0002	0·0010	0·0043	0·0083	0·0184	−0·0068
a_{13}	0·0005	0·0011	0·0023	0·0041	0·0067	0·0082	0·0079	0·0025
a_{14}	−0·0003	−0·0007	−0·0017	−0·0037	−0·0086	−0·0135	−0·0212	0·0039
a_{15}	0·0000	0·0000	0·0001	0·0007	0·0029	0·0058	0·0121	−0·0061
a_{16}	0·0001	0·0003	0·0008	0·0017	0·0039	0·0060	0·0068	0·0021
a_{17}	−0·0001	−0·0002	−0·0005	−0·0013	−0·0034	−0·0057	−0·0160	0·0037
								−0·0055
								0·0018

TABLE 1. Numerical results for the flux k, the propagation velocity W, and the Fourier coefficients a_0–a_{17} of the series $f(t,\alpha) = \sum_{n=0}^{\infty} a_n(\alpha) \cos nt$ for the core boundary ∂A (for parameter values $\alpha \in (0, \surd 2]$)

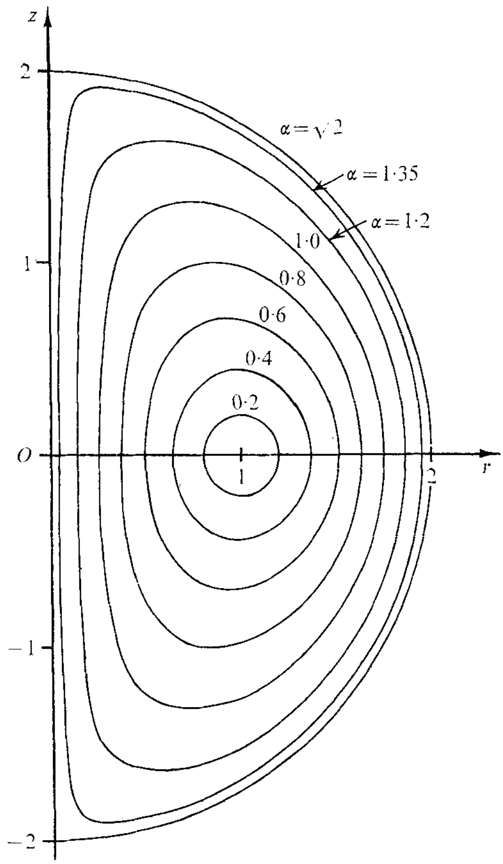

FIGURE 3. The boundary ∂A, of a vortex ring specified by the parameter α, is found numerically, and shown for typical values of $\alpha \in (0, \sqrt{2}]$.

3. The numerical results

First we give a brief description of the program. As was said before, the program modelled equations (2.19*) applied to the problem posed by equations (2.13)–(2.15). No explicit simple formulae were available for calculating $\partial P_\alpha / \partial X_j$ so these derivatives were approximated by $\{P_\alpha(X_j + \Delta) - P_\alpha(X_j)\}/\Delta$ (for a value of $\Delta \doteqdot 0{\cdot}008$). Since most of the computing time was taken up in each evaluation of $P_\alpha(\mathbf{X})$ (approximately 12 s for each evaluation), it was more efficient to replace (2.19a) by (2.19c); that is, use (2.19*), where the same approximation to the matrix $[\partial P_\alpha / \partial X_j(t_i)]$ is used, for several iterations in the sequence $n = 2, 3, \ldots$. Providing that the initial guess $\mathbf{X}^1$ was within approximately 0·01 of the actual root, this process worked very well. The repeated integral in (2.13) was evaluated by using the trapezium rule with a Romberg extrapolation. The logarithmic singularity at $(\hat{r}, \hat{z}) = (r, z)$ was integrated analytically over a sector of a small circle, and a corresponding small domain about the singularity at (r, z) removed from the numerical integration. The integrand was evaluated by using the relation

$$G(r, \hat{r}, z - \hat{z}) = \hat{r}\{(r + \hat{r})^2 + (z - \hat{z})^2\}^{\frac{1}{2}}\{(1 - \tfrac{1}{2}k^2)\,K(k) - E(k)\},$$

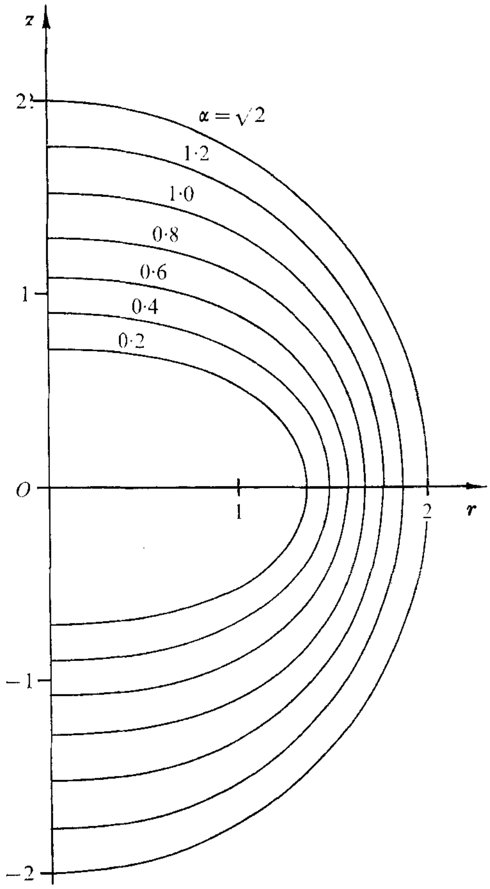

FIGURE 4. The dividing streamline for various parameter values $\alpha \in (0, \sqrt{2}]$. The dividing streamline separates fluid with circulation from the external potential flow.

where $k^2 = 4r\hat{r}/\{(r+\hat{r})^2+(z-\hat{z})^2\}$ is the modulus squared of the usual complete elliptic integrals K and E of the first and second kinds respectively. All calculations were made in double precision to avoid rounding errors.

This program was run on the IBM 360 computer at University College, London. Between 8 and 18 terms in the Fourier series (2.12) were used to approximate ∂A (thus $8 \leqslant N \leqslant 18$ in (2.19*)) for parameter values $0 < \alpha < \sqrt{2}$. The asymptotic results at $\alpha = 0{\cdot}1$ were used as an initial guess when $\alpha = 0{\cdot}1$, and then the results of this calculation used to predict a sufficiently accurate initial guess for the case $\alpha = 0{\cdot}2$, and so on. The results for (k, W, a_n) are given in table 1 and figures 3 and 4. The value $N = 18$ was the largest used since the computational time was approximately 120 min for this case.

The program was written to keep the computational errors in the table values less than $\pm 0{\cdot}0001$. However, for $1 \leqslant \alpha < \sqrt{2}$ the number of terms taken in the series (2.12) was insufficient to ensure this accuracy in the numerical scheme. A cautious estimate would be that the errors in the values of a_n are of the order of the last coefficient given. However, tests made with different values of N

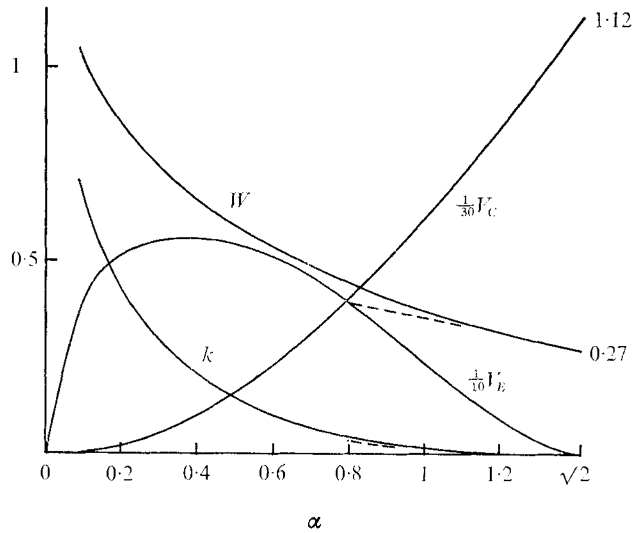

FIGURE 5. The propagation velocity W, flux k, core volume V_c and volume of entrained fluid V_e for parameter values $\alpha \in (0, \sqrt{2}]$. The asymptotic results of Norbury (1973) are shown for W and k as dotted lines.

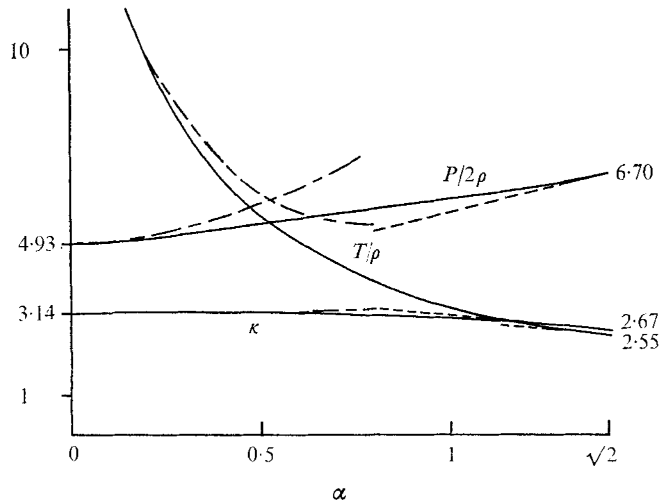

FIGURE 6. The kinetic energy T, circulation κ and fluid impulse P for parameter values $\alpha \in (0, \sqrt{2}]$ (ρ is the fluid density). The asymptotic results are shown as dotted curves: ---, Fraenkel; - - - -, Norbury.

indicate that errors due to the approximation $a_n = 0$ ($n \geqslant 18$) affect the values of k, W, a_0, a_1, ..., a_{10} very little. These values are probably still accurate to within $\pm 0{\cdot}0001$.

The well-behaved numerical convergence suggests that the scheme does find the correct values for k, W, a_0, a_1, ... We also have several independent checks on the accuracy of this numerical scheme. For $\alpha \to 0$ we have the asymptotic results of Fraenkel (1972, p. 132), in particular equations (6.16) and (6.19). The

α ...	0·2	0·4	0·6	0·8	1·0	1·2	$\sqrt{2}$
A	0·1257	0·5027	1·1310	2·0106	3·1416	4·5239	2π
B	0·1256	0·5028	1·1311	2·0105	3·1414	4·5240	
κ	3·1385	3·1261	3·0882	3·0231	2·9363	2·8274	8/3
P	10·1259	10·6966	11·2808	11·7532	12·1837	12·6703	$64\pi/15$
T	9·85	6·58	5·02	3·99	3·29	2·82	$256\pi/315$
V_e	5·1438	5·5864	5·0470	3·9022	2·4368	0·9558	0
V_c	0·7888	3·1426	6·9854	12·1565	18·4495	25·5814	$32\pi/3$
A_0	0·9811	1·1574	1·3223	1·4926	1·6650	1·8345	2·0
A_2	−0·3184	−0·2880	−0·2512	−0·1922	−0·1183	−0·0434	0
A_4	0·0571	0·0340	0·0098	−0·0119	−0·0223	−0·0138	0
A_6	0·0059	0·0002	0·0045	0·0029	−0·0047	−0·0061	0
A_8	0·0004	−0·0015	−0·0009	0·0016	−0·0006	−0·0025	0
A_{10}	0·0010	0·0004	−0·0005	0·0002	0·0000	−0·0006	0

TABLE 2. Numerical results for B, the area of the core (A is the exact result for comparison), the circulation κ, the fluid impulse P, the kinetic energy T, the volume V_e of irrotational fluid carried along with the core, the volume V_c of rotational fluid in the core, and the coefficients A_{2n} of the Fourier series $\rho(\theta,\alpha) = \sum_{n=0}^{\infty} A_{2n}(\alpha)\cos 2n\theta$ describing the dividing streamline $\psi = 0$ for parameter values $\alpha \in (0, \sqrt{2}]$.

α ...	0·2	0·4	0·6	0·8
a_0	0·1999	0·3992	0·596	0·788
a_1	−0·0005	−0·0059	−0·0206	−0·046
a_2	−0·0068	−0·038	−0·096	−0·171
a_3	0·0005	0·0059	0·0206	0·046
W	0·8508	0·6603	0·540	0·45

TABLE 3. For comparison, values for some of the variables of table 1 based upon the asymptotic formulae of Fraenkel (1972)

values in table 3 were calculated from these formulae, and can be directly compared with those of table 1. The good agreement at $\alpha = 0{\cdot}2$ of the numerical and asymptotic results makes it plausible that both are accurate representations of the actual values of the solution there, and that the numerical scheme is sound. Thus we see that these approximate formulae, which we know are valid approximations for $\alpha \to 0$, are useful approximations for quite large values of α. The numerical and asymptotic descriptions of the core boundary are shown in figure 7 for $\alpha = 0{\cdot}8$, at which value of α the asymptotic formulae are clearly becoming inaccurate, particularly near $r = 0$.

For $\alpha \to \sqrt{2}$ we have corresponding asymptotic results. These are (for (ρ,θ) the usual spherical co-ordinates, and with $\bar{\alpha} = \sqrt{2}-\alpha$)

$$\partial A: \rho = a\left\{1 - \tfrac{1}{8}\bar{\alpha}^2\left(\frac{1}{2\sin^2\theta} + \frac{5}{4}\sum_{n=0}^{\infty}\frac{4n+3}{(2n-1)(2n+1)(2n+2)}\frac{dP_{2n+1}(\cos\theta)}{d\cos\theta}\right) + \dots\right\}$$

$$\text{for} \quad \bar{\alpha}^{\frac{2}{3}} \prec \sin\theta\dagger$$

† We use the order notation of Hardy: $f \preccurlyeq g$ if $f(\epsilon) = O\{g(\epsilon)\}$ as $\epsilon \to 0$, $f \prec g$ if $f = o\{g\}$ as $\epsilon \to 0$.

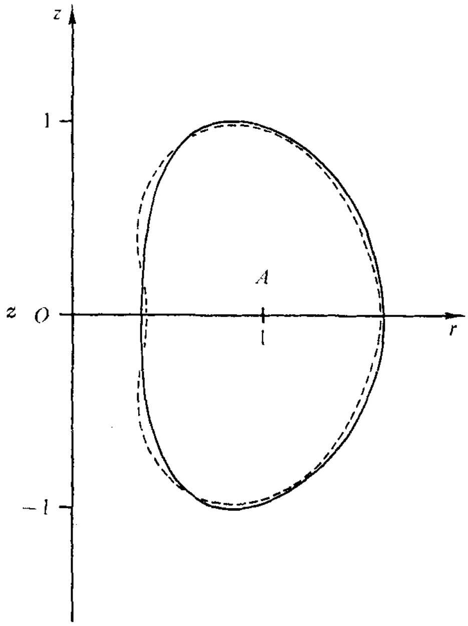

FIGURE 7. The core boundary ∂A for the parameter value $\alpha = 0{\cdot}8$. The dotted curve is the approximate curve found by Fraenkel (1972), which is clearly inaccurate near the axis $r = 0$. For $\alpha = 0{\cdot}6$ the approximate curve of Fraenkel (1972) is less than 0·01 from the numerical curve, except near $t = \frac{3}{4}\pi$, where the error is about 0·03. For $\alpha < 0{\cdot}5$ the differences are less than 0·01.

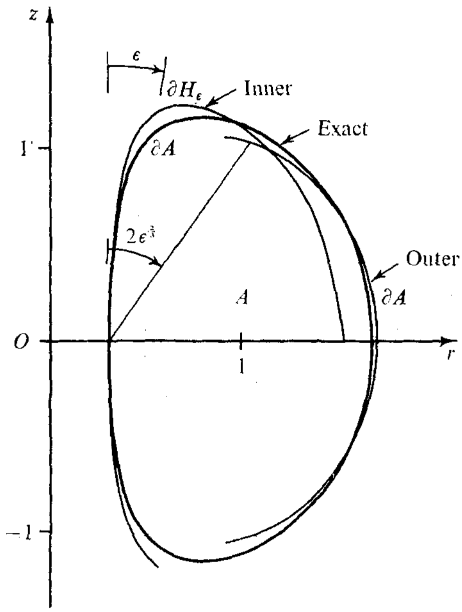

FIGURE 8. The core boundary ∂A for the parameter value $\alpha = 0{\cdot}9$. The asymptotic results of Norbury (1973) are also shown for a parameter value $\epsilon = \overline{\alpha}/2\sqrt{2}$ and a length scale of $a \doteqdot 2(1-\epsilon)$, the appropriate values for the vortex ring shown, where the vorticity constant $\Omega = \alpha^{-2}$.

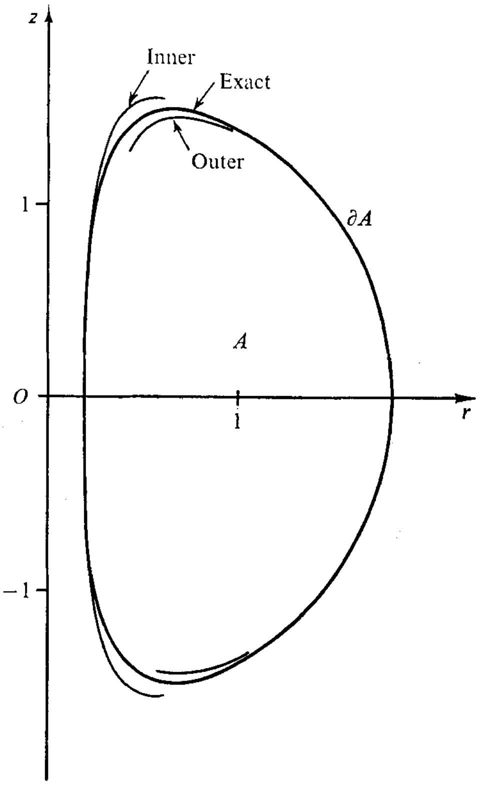

FIGURE 9. The core boundary ∂A for $\alpha = 1{\cdot}1$. For comparison the asymptotic results of Norbury (1973) are used ($\epsilon \doteqdot 0{\cdot}11, a \doteqdot 1{\cdot}78$) to give the 'outer' and 'inner' approximations.

(where $a = 2\{1-\bar{\alpha}/2\sqrt{2}+\ldots\}$), and

$$\rho = a2^{-\frac{1}{2}}\{1 \pm [1-\bar{\alpha}^2/2\sin^2\theta]^{\frac{1}{2}}\}^{\frac{1}{2}}+\ldots\} \quad \text{for} \quad \sin\theta \geqslant \bar{\alpha}/\sqrt{2} \quad \text{and} \quad \rho - a \ngtr \bar{\alpha}^{\frac{2}{3}},$$

$$W = \tfrac{2}{15}(a^2/\alpha^2) = \tfrac{4}{15}\{1+(\bar{\alpha}/\sqrt{2})+\ldots\}, \quad k = \bar{\alpha}^2/10+\ldots.$$

Because of the singular nature of this limiting process $\alpha \to \sqrt{2}$,when the vortex core, which is topologically equivalent to a (doubly connected) torus, tends to a (simply connected) sphere, we might feel that these asymptotic fomulae would be applicable only in a very small region $\sqrt{2} \geqslant \alpha \geqslant \alpha_2$. However, the agreement with the numerical results at $\alpha = 0{\cdot}9$, which is shown in figure 8, is still quite good. The agreement between the numerical and asymptotic results when $\alpha = 1{\cdot}1$ is shown in figure 9, while the numerical results for $\alpha = 1{\cdot}3$ were indistinguishable from the corresponding asymptotic results within the accuracy of the computation. For $\alpha = 1{\cdot}35$, the largest value of α for which the program was run, the numerical solution coincides with the interior streamline of Hill's vortex, with $a \doteqdot 1{\cdot}954$, to the accuracy of figure 3.

Another independent check is the set of results for $\alpha = \sqrt{2}$, which are obtained from the known Hill's vortex. The values in table 1 for $\alpha = \sqrt{2}$ are accurate to within 0·0001, and the convergence of the numerical results across table 1, for each a_i as $\alpha \to \sqrt{2}$, lends more weight to the suggestion that the numerical (and asymptotic) results accurately approximate the correct values.

Various properties of the vortex ring, including the circulation, fluid impulse, kinetic energy, etc., can be calculated from the values in table 1 and the values of these properties are given in table 2. Also included in table 2 is a description of the dividing stream surface (actually the equation

$$\rho = \sum_{n=0}^{\infty} A_{2n} \cos 2n\theta$$

of the dividing streamline, which is the intersection of this stream surface with a meridional plane) and the values of the volume of fluid inside the dividing stream surface and exterior to the vortex core; that is, the irrotational fluid with circulation that is carried along with the vortex core through the exterior potential flow. The results are shown in figures 3–6.

Comparisons with the asymptotic results (shown as dashed lines) were made using the formulae (6.15), (6.17) and (6.18) of Fraenkel (1972) for $\alpha \to 0$ and the following formulae for $\bar{\alpha} = \sqrt{2} - \alpha \to 0$:

$$\text{circulation} \equiv \kappa = \tfrac{1}{3}a^3\{1 + \bar{\alpha}\sqrt{2} - \tfrac{3}{16}\bar{\alpha}^2 \ln(8\sqrt{2}/\bar{\alpha}) + c\bar{\alpha}^2 + \ldots\} \quad (c \doteqdot 1{\cdot}69),$$

$$\frac{\text{fluid impulse}}{\text{fluid density}} \equiv P = \frac{2\pi a^5}{15}\{1 + \bar{\alpha}\sqrt{2} + \tfrac{141}{64}\bar{\alpha}^2 + \ldots\},$$

$$\frac{\text{kinetic energy}}{\text{fluid density}} \equiv T = \frac{2\pi a^7}{315}\{1 + 2\sqrt{(2)}\bar{\alpha} + \tfrac{383}{64}\bar{\alpha}^2 + \ldots\},$$

where $$a = 2\{1 - \bar{\alpha}/2\sqrt{(2)} + O(\bar{\alpha}^2 \ln \bar{\alpha})\}.$$

It is our inability to obtain the terms $\bar{\alpha}^2 \ln \bar{\alpha}$ and $\bar{\alpha}^2$ in the expansion of a which prevents us from obtaining, in this notation, the complete expansions up to $O(\bar{\alpha}^2)$ for comparison with the numerical results. If we estimate a, using the numerical results for W and the relation $W = 2a^2/15\alpha^2$, then the asymptotic and numerical results for κ, P and T differ by less than 1 % for $\alpha \geqslant 0{\cdot}9$.

We have two other checks on the numerical results: first a check on the integration routine used in table 2. Exact values of the area of cross-section A of the core are compared with numerical estimates B, given in table 2. We also applied the formula $\partial T/\partial P = W$ with the circulation held constant to check both the asymptotic and numerical results. (This formula is produced in Norbury (1973).)

Finally we give a résumé of the dimensional variables so that the results of the graphs and tables may be readily converted to useful physical quantities. We have taken the vorticity constant Ω, the ring radius L and the mean core radius αL as given. The propagation velocity is thus given by $W = \Omega L^2 \alpha^2 \overline{W}$, where $\overline{W}$ is the non-dimensionalized speed given in the tables and graph. The flux of fluid between the axis and the core boundary is $k = \Omega L^4 \alpha^2 \bar{k}$, where $\bar{k}$ is given in the results. The various lengths, areas, volumes have been non-dimensionalized by L, L^2 and L^3 respectively. We also have the circulation $\kappa = \Omega L^3 \alpha^2 \bar{\kappa}$, the fluid impulse $P = \rho \Omega L^5 \alpha^2 \bar{P}$, and the total kinetic energy of the motion $T = \rho\Omega^2 L^7 \alpha^4 \bar{T}$, where ρ is the fluid density, and $\bar{\kappa}$, $\bar{P}$, $\bar{T}$ are the quantities in the table and the graph.

The author thanks Mr L. E. Fraenkel, D.A.M.T.P., Cambridge for his assistance as supervisor, and the Commonwealth Scientific and Industrial Research Organisation of Australia for their grant while the author was in Cambridge.

REFERENCES

FRAENKEL, L. E. 1970 On steady vortex rings of small cross-section in an ideal fluid. *Proc. Roy. Soc.* A **316**, 29.

FRAENKEL, L. E. 1972 Examples of steady vortex rings of small cross-section in an ideal fluid. *J. Fluid Mech.* **51**, 119.

NORBURY, J. 1972 A steady vortex ring close to Hill's spherical vortex. *Proc. Camb. Phil. Soc.* **72**, 253.

NORBURY, J. 1973 Asymptotic theory for steady vortex rings close to Hill's spherical vortex. To be submitted to *Proc. Roy. Soc.* A.